Electronic Supplementary Material (ESI) for ChemComm.
This journal is © The Royal Society of Chemistry 2019

**Supplementary Information for**

# The effect of oxidation states of supported oxides on catalytic activity: CO oxidation studies on Pt/cobalt oxide

Hee Chan Song,[ac] Seungtaeg Oh,[de] Sang Hoon Kim,[fg] Si Woo Lee,[bc] Song Yi Moon,[bc] Hanseul Choi,[bc] Soo-Hyun Kim,[h] Yongman Kim,[ac] Jihun Oh*[ade] and Jeong Young Park*[abc]

[a] Graduate School of EEWS, KAIST, Daejeon 34141, Republic of Korea.

[b] Department of Chemistry, KAIST, Daejeon 34141, Republic of Korea.

[c] Center for Nanomaterials and Chemical Reactions, Institute for Basic Science (IBS), Daejeon 34141, Korea.

[d] Department of Materials Science and Engineering, KAIST, Daejeon 34141, Republic of Korea.

[e] KI Institute for NanoCentury, KAIST, Daejeon 34141, Republic of Korea.

[f] Materials Architecturing Research Centre, Korea Institute of Science and Technology (KIST), Seoul 136-791, Republic of Korea.

[g] Division of IT-NT, KIST School, University of Science and Technology (UST), Daejeon 305-333, Republic of Korea.

[h] School of Materials Science and Engineering, Yeungnam University, Gyeongsangbuk-do 38541, Republic of Korea.

* Corresponding author: E-mail: jeongypark@kaist.ac.kr (J.Y.P.), jihun.oh@kaist.ac.kr (J.O.)

## Experimental details

### 1.1 Atomic layer deposition of $CoO_x$ on Si wafers.

Cobalt oxide ($CoO_x$) thin films were deposited by atomic layer deposition (ALD) on Si (100) wafers. The $CoO_x$ films were deposited using a travelling-wave type ALD reactor (Lucida-D100, NCD Technology) with bis(1,4-di-iso-propyl-1,4-diazabutadiene)cobalt [$C_{16}H_{32}N_4Co$, $Co(dpdab)_2$] and oxygen ($O_2$) as the precursor and reactant, respectively. One ALD cycle is made up of 10 s of Co precursor pulsing, 10 s of $N_2$ purging, and 10 s of oxygen reactant pulsing, followed by 10 s of $N_2$ purging to ensure self-limiting ALD growth of the $CoO_x$ films. The Co precursor line was kept at 373 K to prevent any possible condensation of the precursor during the reaction. After every precursor and reactant pulse, 100 sccm of $N_2$ was injected into the ALD chamber as a purging gas to eliminate any residual chemicals and reaction by-products. The phase of the $CoO_x$ film was then determined by the temperature in the ALD chamber. $CoO_x$ films with CoO and $Co_3O_4$ phases are formed with deposition temperatures of 423 and 573 K, respectively. The growth rates of the ALD $CoO_x$ films deposited at 423 and 573 K were observed to be 0.039 and 1.13 nm/cycle, respectively. In this work, the thickness of all the ALD $CoO_x$ films was set to about 55 nm.

### 1.2 Pt nanoparticle deposition on the $SiO_2$, CoO, and $Co_3O_4$ thin films via the Langmuir–Blodgett technique and arc plasma deposition.

Pt nanoparticles (PtNPs) were synthesized using one-pot polyol reduction and arc plasma deposition (APD) to investigate the effect of the organic capping agent on the interface between the metal and oxide thin films. First, the colloidal PtNPs were synthesized via the one-pot polyol reduction method. In detail, for the 1.9 nm PtNPs, 100 mg of $H_2PtCl_6{\cdot}6H_2O$, and 5 mL of 0.5 M NaOH were dissolved in 10 mL of ethylene glycol (EG); this solution was refluxed at 433 K for 2 hours with argon purging. After that, 20.3 mg of poly(N-vinylpyrrolidone) (PVP, MW = 29,000) was added as a stabilizer. In the case of the 5.6 nm PtNPs, a solution of 120 mg of tetramethyl-ammonium bromide [$N^+(CH_3)4Br^-$], 20 mg of ammonium tetrachloroplatinate (II) [$(NH_4)_2PtCl_6$], 100 mg of PVP (MW = 29,000), and 10 mL of EG was heated at 453 K for 20 min. Using TEM analysis, the size and topography of the 1.9 and 5.6 nm PtNPs were characterized (Fig. 1). Both the 1.9 and 5.6 nm PtNPs were diluted in 20 ml of ethanol and sonicated for 10 min to prepare the Pt suspension for the Langmuir–Blodgett process without drying. A chloroform solution of 750 µL of the Pt suspension (Pt : chloroform = 1 : 1) was dropped on the water surface in the Langmuir–Blodgett trough (611 Nima Technology) at room temperature. The initial surface pressure was adjusted to zero before and after dropping the Pt suspension. A two-dimensional film of PtNPs on the prepared substrates was formed by compressing the layer of PtNPs on the water surface with a barrier speed of 10 $cm^2$/min to the target surface pressures of 12 and 15 mN/m for the 1.9 and 5.6 nm PtNPs, respectively. The lifting rate of the substrate beneath the water was 1 mm/min. To prepare the non-capped Pt samples, a coaxial pulsed arc plasma deposition system (ULVAC, ARL-300) was used to deposit the PtNPs onto the three different metal oxides at room temperature under vacuum, *i.e.*, about $10^{-6}$ Torr. The size of the PtNPs can be manipulated by changing the arc voltage and the number of plasma pulses. To fabricate the 2 nm PtNPs, the arc voltage and the condenser capacity were set at 100 V and 1080, respectively. The number of plasma pulses was 30 shots.

## Characterization

The size distribution and morphology of the synthesized PtNPs were evaluated using cross-section high resolution transmission electron microscopy (HR-TEM, Titan Cubed G2 60-300 (FEI)) and scanning transmission electron microscopy and high-angle annular dark field (STEM-HAADF, Titan Cubed G2 60-300 (FEI). The TEM samples were prepared by cutting cross sections of the 5.6 nm PtNPs on $Co_3O_4$ using the focused ion beam technique (FIB, Helios Nanolab™ 450 F1). The morphology of the PtNPs on cobalt oxide catalysts was confirmed using scanning electron microscopy (SEM, Magellan 400 (FEI)). The chemical states of the platinum (Pt 4f) and cobalt oxide (Co 2p) were identified using X-ray photoelectron spectroscopy (XPS, Thermo VG Scientific Sigma Probe with an Al Kα X-ray source (1486.3 eV)) with an energy resolution of 0.5 eV full width at half maximum under ultra-high vacuum ($10^{-10}$ Torr). All the binding energies were calibrated to the C 1s peak at 284.8 eV. The crystal structures of the CoO and $Co_3O_4$ thin films were revealed using X-ray diffraction (Rigaku D/MAX 2500 at 40 kV, 300 mA) patterns with Cu K radiation over the 2Θ range of 10–80°.

## CO oxidation and kinetics study

The catalytic performance was measured in an ultra-high vacuum chamber (1 L) with a base pressure of $10^{-8}$ Torr evacuated using rotary and turbo molecular pumps. After evacuation, reactant gases of 40 Torr of CO and 100 Torr of $O_2$ and 620 Torr of He as the balancing gas were filled into the batch chamber. The mixed gases in the reactor were circulated through the reaction line using a Metal Bellows recirculation pump (MB-41) at 2 L min$^{-1}$. To detect the reactants and products, a DS 6200 gas chromatograph was used with a thermal conductivity detector; a 6 ft. × 1/8 in. SS molecular sieve 5A was used to separate the reactants, *i.e.*, CO and $O_2$, and the product, *i.e.*, $CO_2$. The CO conversion was measured dependent on the reaction temperature (453–523 K). The reaction rates, *i.e.*, turnover frequencies (TOF), were obtained in units of $CO_2$ produced per Pt active surface site per reaction time (sec) as shown in the following equation:

$$Turnover\ \ frequency\ \ (TOF) = \frac{Turnover\ \ number\ (TON)}{Reaction\ \ time} = \frac{(CO\ conversion\ ) \times \frac{P_{CO} V}{RT} \times N_A}{Pt\ active\ \ surface\ \ site\ \times Reaction\ \ time}$$

All the reaction data were obtained at low conversion, *i.e.*, CO conversion less than 20%, presuming that the initial reaction rate was in a kinetically controlled regime. The number of Pt active sites was obtained from the surface areas of SEM images of the 1.9 and 5.6 nm PtNPs on CoO and $Co_3O_4$ (Fig. S3). For the APD Pt samples, we refer to reference (26). Kinetic experiments of CO oxidation on the 5.6 nm PtNPs on $Co_3O_4$ were performed at 513 K with a partial pressure of CO (3.2 ~ 160 Torr) with 100 Tor of $O_2$ and a partial pressure of $O_2$ (10 ~ 82 Torr) with 40 Torr of CO.

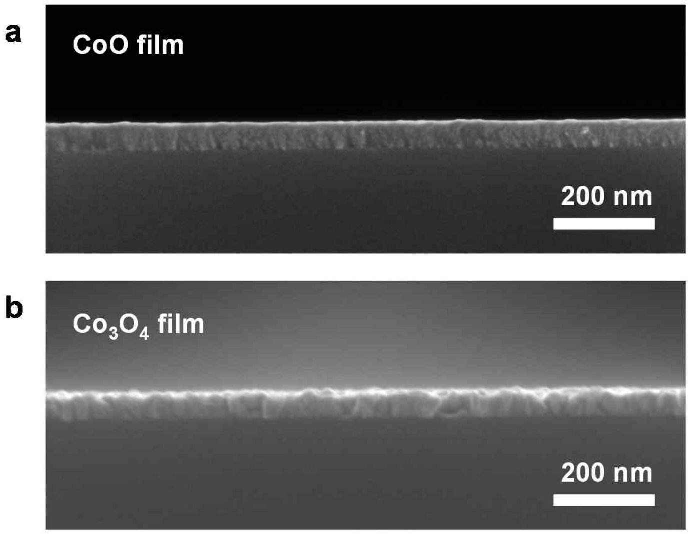

**Fig. S1** SEM cross section images of the (a) CoO and (b) $Co_3O_4$ thin films fabricated via atomic layer deposition.

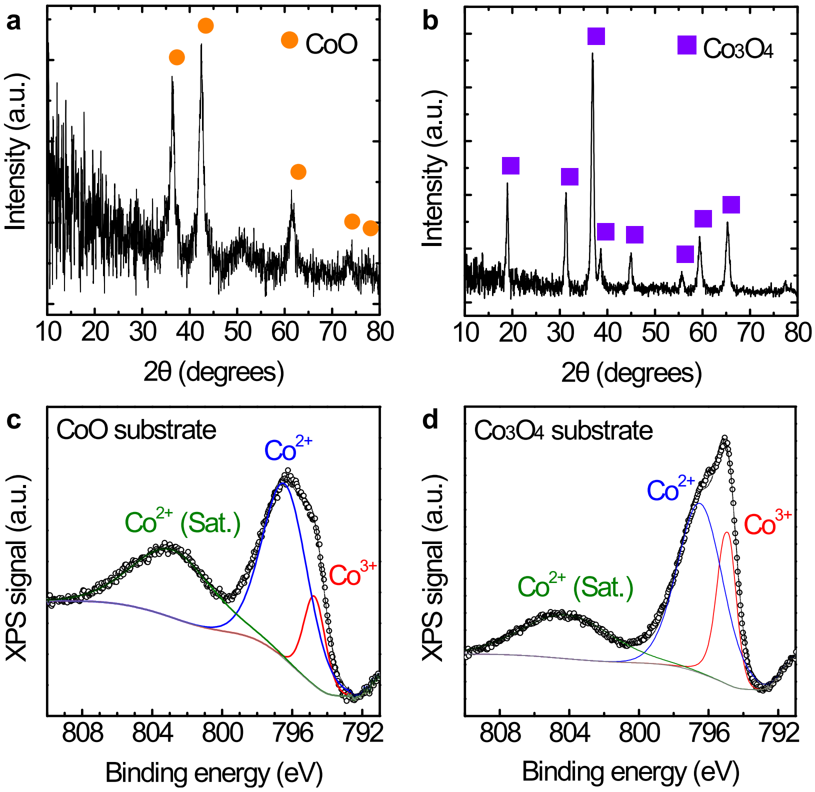

**Fig. S2** XRD patterns and XPS spectra of Co 2p for the (a, c) CoO and (b, d) $Co_3O_4$ films.

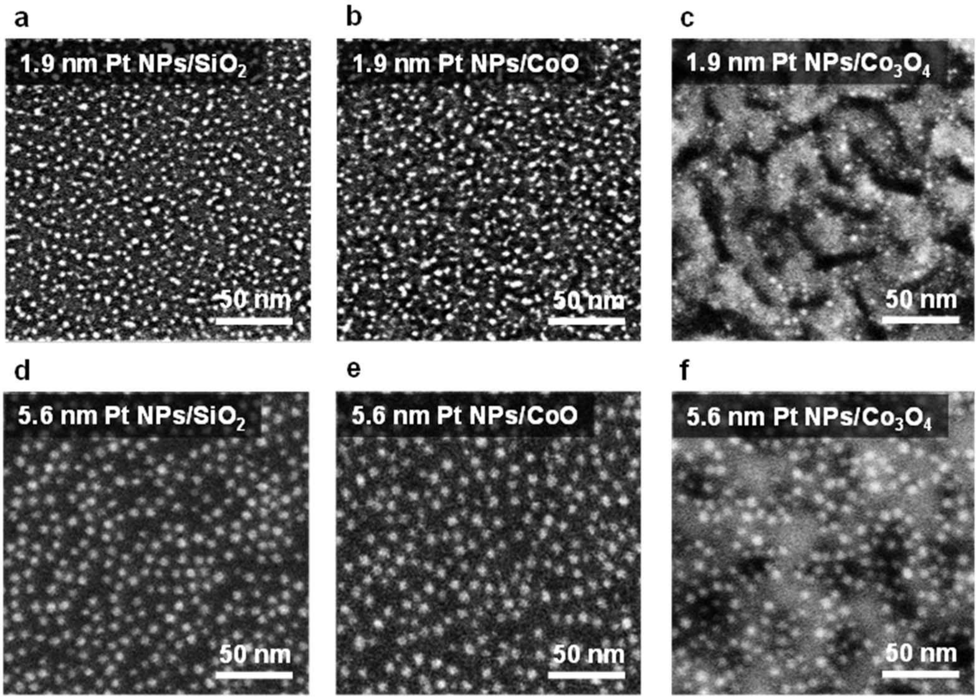

**Fig. S3** SEM images of the 1.9 and 5.6 nm PtNPs on (a, d) $SiO_2$, (b, d) CoO, and (c, f) $Co_3O_4$ substrates.

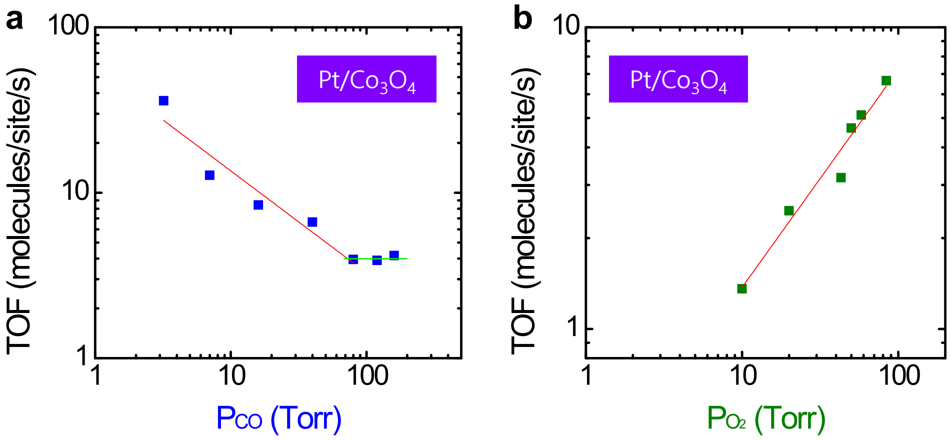

**Fig. S4** Kinetic study for CO oxidation on the 5.6 nm PtNPs supported on $Co_3O_4$ at 513 K as a function of (a) CO pressure and (b) $O_2$ pressure.

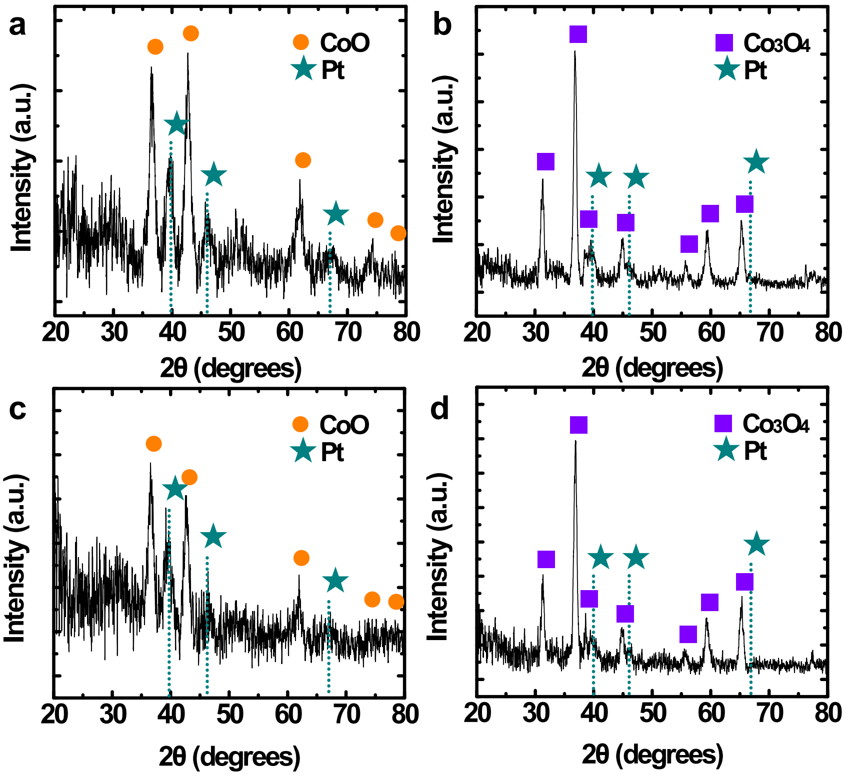

**Fig. S5** XRD patterns of the 5.6 nm PtNPs on CoO and $Co_3O_4$ thin films (a, b) before and (c, d) after the CO oxidation reaction.

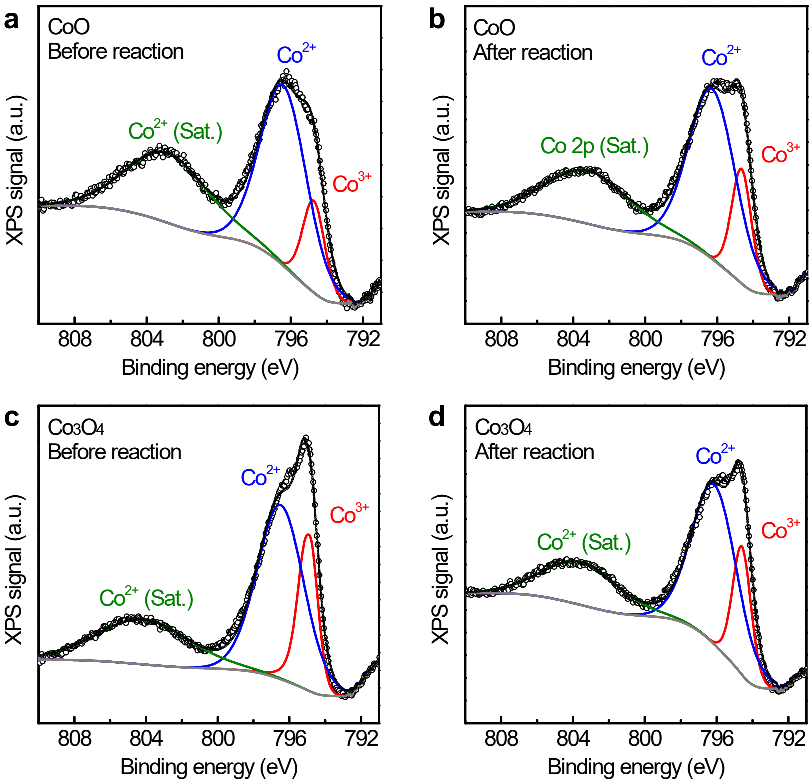

**Fig. S6** XPS spectra of Co 2p for the CoO and $Co_3O_4$ thin films (a, c) before and (b, d) after the CO oxidation reaction.

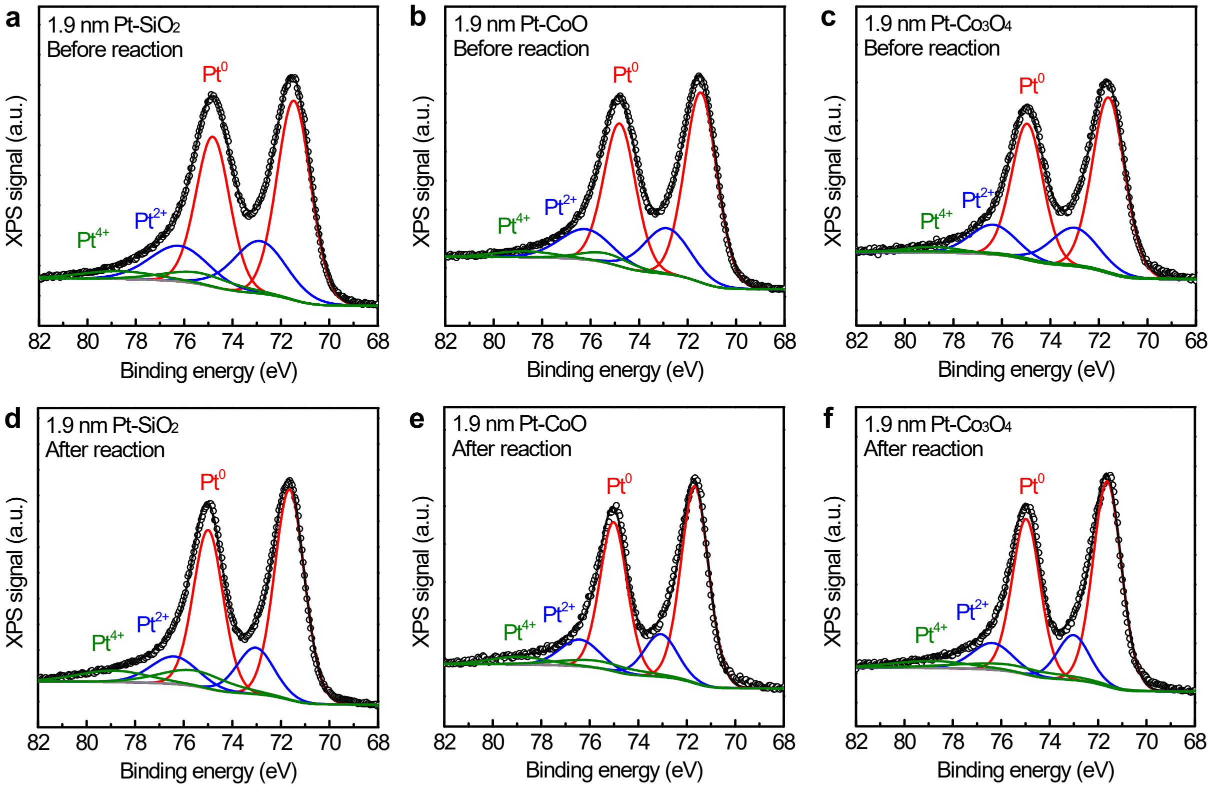

**Fig. S7** XPS spectra of Pt 4f for the 1.9 nm PtNPs on $SiO_2$, CoO, or $Co_3O_4$ thin films (a, b, c) before and (d, e, f) after the CO oxidation reaction.

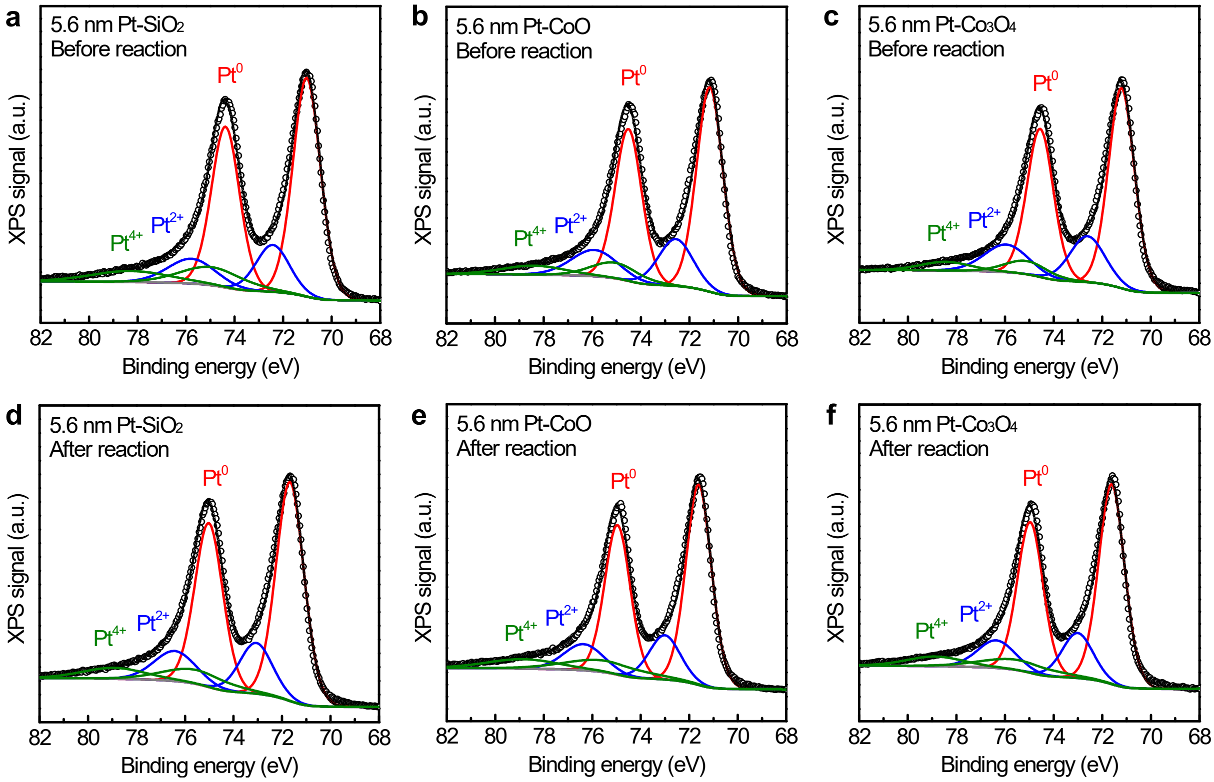

**Fig. S8** XPS spectra of Pt 4f for the 5.6 nm PtNPs on $SiO_2$, CoO, or $Co_3O_4$ thin films (a, b, c) before and (d, e, f) after the CO oxidation reaction.

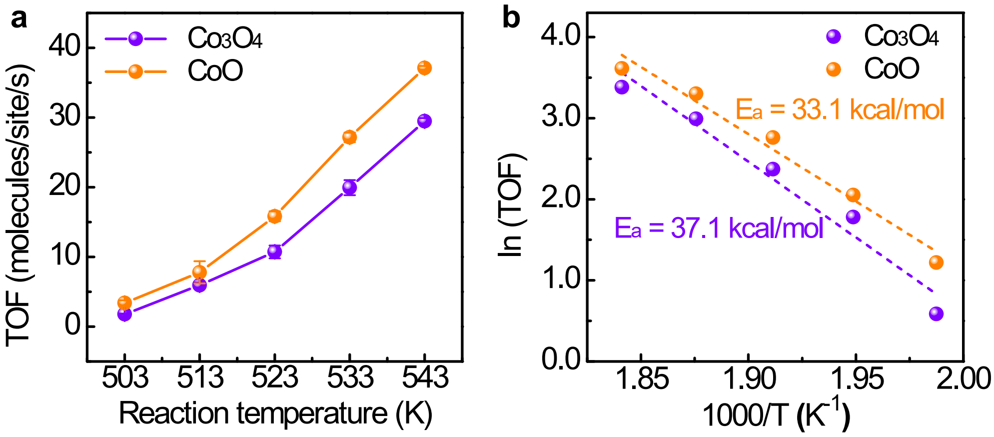

**Fig. S9** TOF and Arrhenius plot for CO oxidation on the CoO and $Co_3O_4$ substrates.